Perfectly planar boronyl boroxine D3h B6O6: A boron oxide analog of boroxine and benzene

Da-Zhi Li, Hui Bai, Qiang Chen, Haigang Lu, Hua-Jin Zhai et al.

Citation: J. Chem. Phys. **138**, 244304 (2013); doi: 10.1063/1.4811330
View online: http://dx.doi.org/10.1063/1.4811330
View Table of Contents: http://jcp.aip.org/resource/1/JCPSA6/v138/i24
Published by the AIP Publishing LLC.

THE JOURNAL OF CHEMICAL PHYSICS **138**, 244304 (2013)

Perfectly planar boronyl boroxine D_{3h} B_6O_6: A boron oxide analog of boroxine and benzene

Da-Zhi Li,[1,2,a)] Hui Bai,[1,a)] Qiang Chen,[1] Haigang Lu,[1] Hua-Jin Zhai,[1,b)] and Si-Dian Li[1,b)]
[1]*Institute of Molecular Science, Shanxi University, Taiyuan 030006, Shanxi, People's Republic of China*
[2]*Department of Chemistry and Chemical Engineering, Binzhou University, Binzhou 256603, Shandong, People's Republic of China*

(Received 2 April 2013; accepted 3 June 2013; published online 25 June 2013)

Inorganic benzene-like compounds such as boroxine and borazine are of interest in chemistry. Here we report on theoretical prediction of a new member of the inorganic benzene family: boronyl boroxine. This perfectly planar D_{3h} B_6O_6 (**1**, $^1A_1'$) cluster is identified as the global minimum of the system at density functional theory (B3LYP) and molecular orbital theory levels, which lies at least ~20 kcal/mol lower in energy than alternative structures. It can be formulated as $B_3O_3(BO)_3$ and features a boroxol B_3O_3 ring as the core with three boronyl (BO) groups attached terminally, closely resembling boroxine and obtainable from the latter via isovalent BO/H substitution. Detailed bonding analyses reveal weak π aromaticity in boronyl boroxine, rendering it a true analog to boroxine and borazine. Upon electron attachment, the slightly distorted C_{2v} $B_6O_6^-$ (**2**, $^2A_2$) anion is also perfectly planar, and its electronic properties are calculated. A huge energy gap (4.83 eV) is predicted for $B_6O_6^-$ (**2**) at B3LYP level, which is characteristic of a stable closed-shell neutral cluster. Similar to benzene, boronyl boroxine is also predicted to be an effective inorganic ligand to form sandwich-type complexes, such as D_{3d} $[B_3O_3(BO)_3]_2Cr$ (**4**, ^1A_g). © *2013 AIP Publishing LLC*. [http://dx.doi.org/10.1063/1.4811330]

I. INTRODUCTION

The past few years have witnessed increasing research activities in boron oxide clusters,[1–18] due primarily to their novel structures and chemical bonding, and to their role in mechanistic understanding of the highly-energetic combustion processes of boron and boranes at a molecular level.[19] Concerted recent experimental and theoretical data have established the isolobal analogy[10–14] between the boronyl (BO) group[20,21] and the H atom, which can both be considered as monovalent σ ligands. This concept provides an unexpected link between boron oxide clusters and boranes,[22] allowing rational design of new boron oxide clusters and boron boronyl complexes. Among boron oxide clusters characterized, the linear $D_{\infty h}$ $B(BO)_2^{0/-}$, triangular D_{3h} $B(BO)_3^{0/-}$, and perfect tetrahedral T_d $B(BO)_4^-$ form a series with a monoboron center attached with terminal boronyl ligands,[10,16] akin to the simplest boranes: $BH_n^{0/-}$ (n = 2–4). The linear-chain $D_{\infty h}$ $B_2(BO)_2^{0/-/2-}$ clusters[11] are relevant to diborene B_2H_2 (and acetylene C_2H_2 as well), in which the B_2 core is attached by two terminal boronyl groups, one on each end. Upon changing the charge state from neutral to anion to dianion, the formal BB bond order in the B_2 core varies from 2 to 2.5 to 3, marking the $B_2(BO)^{2-}$ dianion as the first global-minimum complexes with a true B≡B triple bond. Furthermore, η^2 BO groups are characterized in $B_2(BO)_3^-$ and $B_3(BO)_3^-$ clusters,[12] which each possesses a bridging three-center two-electron B–(BO)–B σ bond that is similar to the τ bond in boranes.[22] Based on the concept of BO/H isolobal analogy, our group has also investigated very recently the boronyl-substituted ethylenes $C_2H_{4-m}(BO)_m$ (m = 1–4) and acetylenes $C_2H_{2-m}(BO)_m$ (m = 1, 2) using density functional theory (DFT), which all prove to be stable species on their potential energy surfaces.[23] Cage-like boron boronyl clusters, $B_n(BO)_n^{2-}$, $CB_{n-1}(BO)_n^-$, and $C_2B_{n-2}(BO)_n$ (n = 5–12), have also been studied theoretically. These are isovalent with each other and represent boronyl analogs of the *closo*-boranes $B_nH_n^{2-}$, monocarboranes $CB_{n-1}H_n^-$, and dicarboranes $C_2B_{n-2}H_n$, respectively.[24]

Boron oxide and boron boronyl clusters that have been studied to date are relatively boron-rich.[1–18] These generally contain a boron cluster core and an appropriate number of boronyl groups attached to it, either terminally or in a bridging fashion. It is anticipated that the composition ratio of B versus O should offer a critical parameter to fine-tune the electronic, structural, and bonding properties of boron oxide clusters. Novel clusters may emerge during the pursuit in this direction. In the current contribution, we report on the discovery of *boronyl boroxine*, D_{3h} B_6O_6 (**1**, $^1A_1'$), a new member of the "inorganic benzene" family. This perfectly planar cluster is identified as the global-minimum structure on the basis of unbiased, extensive global minimum searches. It is at least ~20 kcal/mol lower in energy than alternative structures at both the B3LYP and single-point coupled-cluster with single, double, and perturbative triple excitations (CCSD(T)) levels.

Boronyl boroxine D_{3h} B_6O_6 (**1**, $^1A_1'$) can be formulated as $B_3O_3(BO)_3$: it possesses a boroxol B_3O_3 ring as the core with three BO groups terminally attached to three B atoms, which is structurally and chemically similar to

a)D.-Z. Li and H. Bai contribute equally to this work.
b)Authors to whom correspondence should be addressed. Electronic addresses: hj.zhai@sxu.edu.cn and lisidian@sxu.edu.cn.

boroxine ($B_3O_3H_3$)[25–30] and can be constructed from the latter via isovalent BO/H substitution. Prototypical members of the inorganic benzene family include boroxine and borazine ($B_3N_3H_6$),[30–33] which have received persistent attention both experimentally and theoretically. The present work extends the chemistry of boroxine, and represents as well a new development in boronyl chemistry. Chemical bonding in boronyl boroxine is analyzed using adaptive natural density partitioning (AdNDP),[34] natural resonance theory (NRT), and nucleus independent chemical shift (NICS).[35,36] These collectively confirm that B_6O_6 (**1**) cluster is indeed the boron oxide analog of boroxine with 6π electrons. Weak π aromaticity is revealed for B_6O_6 (**1**), similar to boroxine and borazine.[33] The discrepancy between benzene and boronyl boroxine or boroxine is also analyzed. Furthermore, to explore boronyl boroxine chemistry, we have attempted to design new sandwich-type transition metal complexes, D_{3d} $[B_3O_3X_3]_2Cr$ (X = BO, H). In such complexes, boronyl boroxine or boroxine units, $B_3O_3X_3$ (X = BO, H), are utilized as robust inorganic ligands, similar to the sandwich-type complexes based on benzene or borazine.

II. THEORETICAL METHODS

DFT structural searches for the B_6O_6 cluster were conducted initially using the gradient embedded genetic algorithm (GEGA),[37,38] Coalescence Kick (CK),[39,40] and Basin Hopping[41] global-minimum search programs. The candidate low-lying structures were further optimized and frequency analyses performed at the B3LYP level[42,43] with the 6-311+G(d,p) basis sets, as implemented in the GAUSSIAN 03 program.[44] The relative energies for the low-lying isomers were also refined using CCSD(T)[45–48] at the B3LYP geometries. Born-Oppenheimer molecular dynamics (BOMD) simulations for D_{3h} B_6O_6 (**1**) were performed at 300K for 20 ps to check the dynamic behaviors using the software suite CP2K.[49,50] For the sandwich-type model complexes, the Stuttgart relativistic small core basis set and effective core potential (Stuttgart RSC 1997 ECP)[51] was employed for Cr. The NBO 5.0 program[52] was used to calculate the natural atomic charges.

III. RESULTS

Figure 1 shows the global-minimum structure for the neutral B_6O_6 cluster, D_{3h} (**1**, $^1A_1'$), as identified at both the B3LYP/6-311+G(d,p) and single-point CCSD(T) levels. Its corresponding anion structure, C_{2v} $B_6O_6^-$ (**2**, $^2A_2$), and that of boroxine D_{3h} $B_3O_3H_3$ (**3**, $^1A_1'$) are also shown. Alternative optimized low-lying structures of B_6O_6 at the B3LYP level are depicted in Fig. 2, along with their relative energies at both B3LYP and single-point CCSD(T) levels.

A. Global-minimum B_6O_6 structure

As shown in Figs. 1 and 2, the B_6O_6 (**1**, $^1A_1'$) state with D_{3h} symmetry is clearly the global minimum of the system. This structure appears to be not easy, if not impossible, to conceive *a priori*. Indeed, for such a binary, relatively large system with six B plus six O atoms to self-assemble into this unique, highly-symmetric planar structure, some interesting chemistry has to underlie it. Yet once presented, its connection to the ternary boroxine D_{3h} $B_3O_3H_3$ (**3**, $^1A_1'$) complex is readily recognizable. The analogy suggests that B_6O_6 (**1**) is boronyl boroxine, which can be formulated as $B_3O_3(BO)_3$, that is, a boroxol B_3O_3 core attached with three terminal BO groups. To the best of our knowledge, a similar boron oxide core has not been definitively characterized in prior studies,[1–17] although it is among the possible "guess" structures for some $B_mO_n^+$ cation clusters based on mass spectrometric observations.[18] The BOMD simulations well support the high stability of B_6O_6 (**1**) (see Fig. S1 in the supplementary material).[53] The root-mean-square-deviation (RMSD) and maximum deviation (MaxD) of bonds in B_6O_6 turn out to be only 0.038 and 0.077 Å (on average), respectively, at 300 K with respect to those in its minimum structure, indicating that B_6O_6 possesses a quite rigid global-minimum structure that is dynamically stable under ambient conditions. It is noted that during the BOMD simulations, we were unable to locate any structure that corresponds to a dissociated cluster, let alone any dissociated cluster that is more stable than B_6O_6 (**1**) itself. In fact, the cluster motif and atomic connectivity of B_6O_6 (**1**) do not alter in the simulations, hinting its structural robustness. We have, therefore, calculated the dissociation energies for representative reaction channels at the B3LYP level, as summarized in Table SI in the supplementary material.[53] Clearly, all the proposed dissociation channels are highly endothermic, and the least energy-costly channel requires an energy of ~60 kcal/mol, consistent with the thermodynamic stability of the B_6O_6 (**1**) cluster.

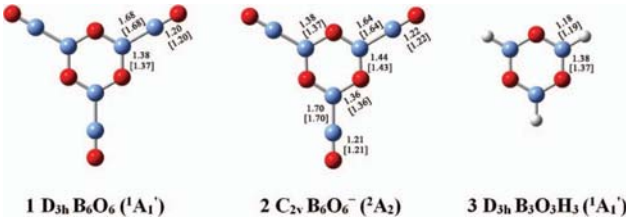

FIG. 1. Optimized structures of boronyl boroxine D_{3h} B_6O_6 (**1**, $^1A_1'$) and its anion C_{2v} $B_6O_6^-$ (**2**, $^2A_2$) at the B3LYP/6-311+G(d,p) level, as compared to that of boroxine D_{3h} $B_3O_3H_3$ (**3**, $^1A_1'$). The bond distances (in Å) are indicated at B3LYP and [PBE1PBE] levels. The B atom is in blue, O in red, and H in gray.

The B−O bond distance within the B_3O_3 ring in B_6O_6 (**1**) is remarkably similar to that in $B_3O_3H_3$ (**3**) at the B3LYP level: r_{B-O} = 1.38 Å in **1** versus r_{B-O} = 1.38 Å in **3**. Also, the B≡O bond distance in **1** is calculated to be $r_{B\equiv O}$ = 1.20 Å, similar to $r_{B\equiv O}$ = 1.20 Å in free BO radical,[21] which indicates that the structural integrity of boronyl groups is well preserved. Note that the calculated structural parameters for **3** are r_{B-O} = 1.38 Å, r_{B-H} = 1.18 Å, ∠BOB = 121°, and ∠OBO = 119° at B3LYP level, in close agreement with the experimental data for boroxine (r_{B-O} = 1.375 ± 0.002 Å, r_{B-H} = 1.192 ± 0.017 Å, and ∠BOB = ∠OBO = 120.00 ± 0.64°).[31] This serves as a valuable benchmark for the

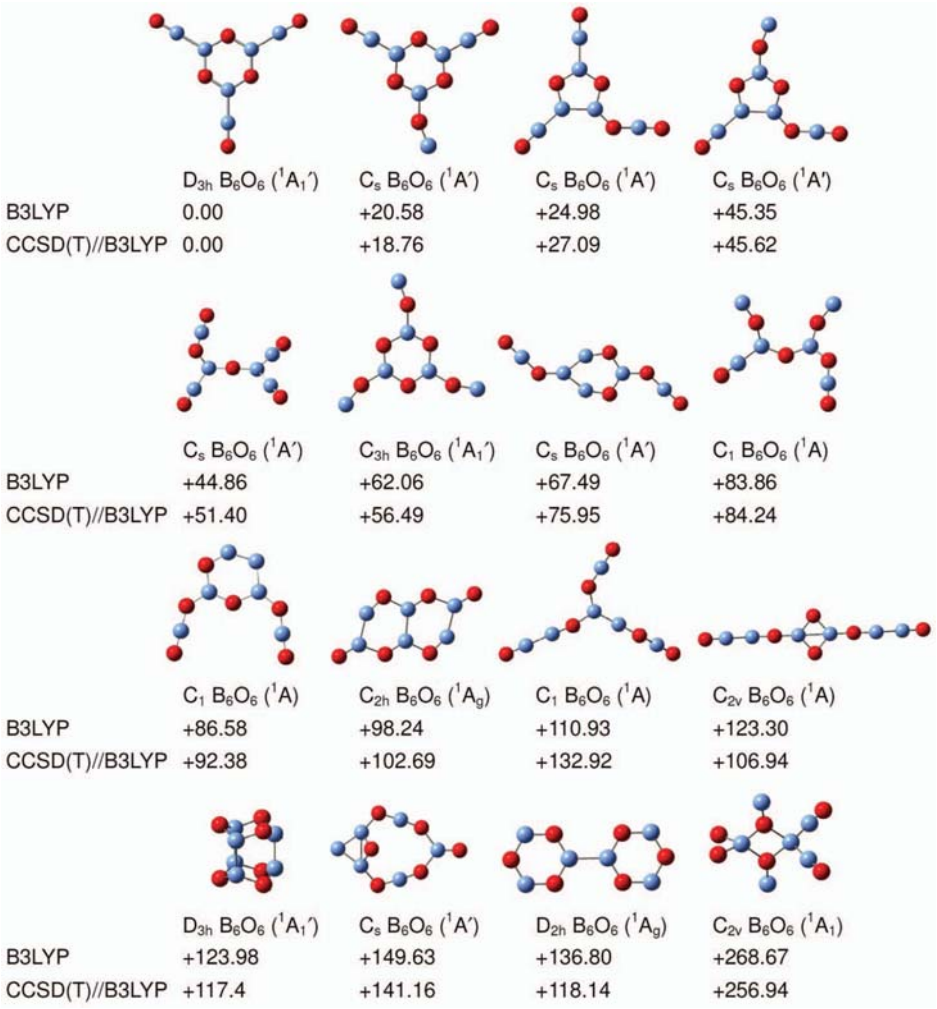

FIG. 2. Representative isomeric structures of B_6O_6 with their relative energies (in kcal/mol) indicated at the B3LYP/6-311+G(d,p) and single-point CCSD(T)//B3LYP/6-311+G(d,p) levels. The B atom is in blue, and O is in red.

B3LYP method. The PBE1PBE calculations generated essentially the same structures (Fig. 1).

Per request of a reviewer, we have run full structural optimization at the CCSD/6-31G(d) and CCSD/6-311+G(d,p) levels and frequency analysis at the CCSD/6-31G(d) level, in order to show that the global-minimum structure **1** at B3LYP remains a true minimum at the CCSD level. The CCSD optimized structures for B_6O_6 (**1**) are depicted in Fig. 3. Note the bond distances at the CCSD/6-31G(d) level (1.21, 1.38, and 1.69 Å) are nearly identical to those at CCSD/6-311+G(d,p) (1.20, 1.38, and 1.69 Å), which are compared to the values of (1.20, 1.38, and 1.68 Å) and (1.20, 1.37, and 1.68 Å), respectively, at the B3LYP/6-311+G(d,p) and PBE1PBE/6-311+G(d,p) levels (Fig. 1).

The minimum vibrational frequency at the CCSD/6-31G(d) level is 62 cm^{-1}, due to the out-of-plane bending of terminal BO groups. This is comparable to those of 62 and 61 cm^{-1} at the B3LYP/6-311+G(d,p) and PBE1PBE/6-311+G(d,p) levels, respectively. All three levels of theory thus concertedly confirm B_6O_6 (**1**) as a true minimum. In addition, we note that B_6O_6 (**1**) is also a true minimum at the MP2/6-311+G(d,p) level, with a minimum vibrational frequency of 62 cm^{-1}. Frequency analysis at the CCSD/6-311+G(d,p) level appears to be too costly for us to pursue at present.

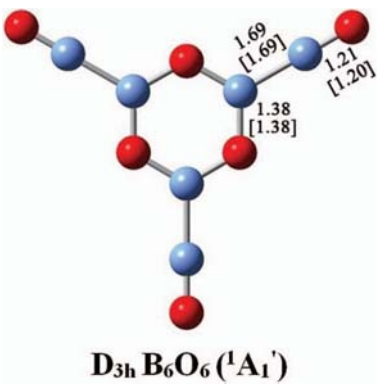

FIG. 3. Optimized structures of boronyl boroxine D_{3h} B_6O_6 (**1**, $^1A_1'$) at the CCSD/6-31G(d) and [CCSD/6-311+G(d,p)] levels. The B atom is in blue, and O is in red.

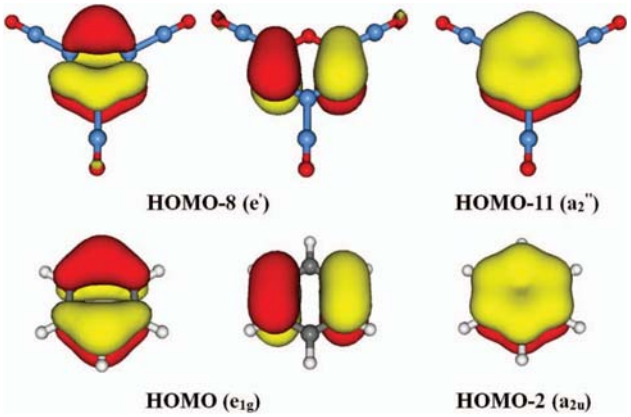

FIG. 4. Comparison of the π molecular orbitals of (top panel) boronyl boroxine D_{3h} B_6O_6 (**1**, $^1A_1'$) with those of (bottom panel) benzene.

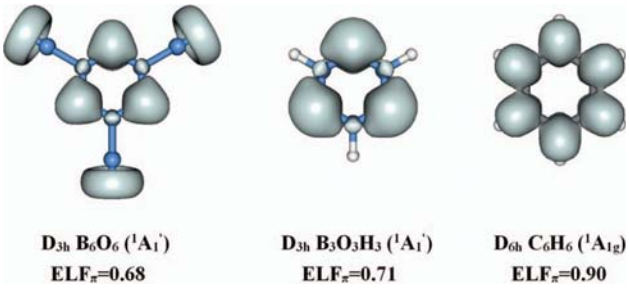

FIG. 5. Electron localization functions (ELFs) of D_{3h} B_6O_6 (**1**), D_{3h} $B_3O_3H_3$ (**3**), and D_{6h} C_6H_6 with the π bifurcation values ELF_π indicated in the interval [0,1], which are indicators of π aromaticity.

B. Isomeric B_6O_6 structures

Among alternative low-lying structures identified for B_6O_6 (Fig. 2), the second lowest isomer, C_s ($^1A'$), is 20.58 and 18.76 kcal/mol, respectively, higher in energy at the B3LYP and single-point CCSD(T) levels, suggesting that the D_{3h} B_6O_6 (**1**, $^1A_1'$) global minimum is well defined on the potential energy surface. The B≡O units in the C_s ($^1A'$) isomeric structure are also well maintained as boronyl groups (with $r_{B\equiv O}$ = 1.20−1.21 Å). Other optimized structures lie even higher above the global minimum (by at least ∼25 kcal/mol). Note that the energetics from B3LYP and single-point CCSD(T) calculations are remarkably consistent with each other (Fig. 2). Actually, in all B_6O_6 structures presented, whenever a BO unit is in a terminal position and attached to a B atom, it can be faithfully classified as a boronyl group with $r_{B\equiv O}$ = 1.20−1.21 Å. The first triplet excitation in B_6O_6 (**1**), via an adiabatic one-electron promotion, leads to the slightly distorted planar C_{2v} B_6O_6 ($^3A_2$) triplet excited state (not shown), which is 5.26 eV above the global minimum (**1**) at the B3LYP level.

IV. DISCUSSION

A. Boronyl boroxine: A boron oxide analog of boroxine and benzene

Boroxine D_{3h} $B_3O_3H_3$ (**3**, $^1A_1'$) as an inorganic analog of benzene in terms of geometry and formal topology of the π molecular orbitals (MOs) has been well known.[25–30] The same is true for boronyl boroxine, D_{3h} $B_3O_3(BO)_3$ (**1**, $^1A_1'$). As shown in Fig. 4 (top panel), there exist three global π MOs in **1**: HOMO−11 (a_2'') and the degenerate HOMO−8 (e') orbitals, which are six-center two-electron (6c-2e) in nature as well, similar to benzene (Fig. 4; bottom panel). Thus, boronyl boroxine formally conforms to the $(4n + 2)$ Hückel rule, rendering it π aromaticity as a new inorganic benzene. However, just as the situation in boroxine and borazine, the main difference in π electron distribution in **1** with respect to benzene is that the π electrons are heavily located on the three oxygen centers in the B_3O_3 boroxol ring, as clearly indicated in the π electron localization functions (π ELFs; Fig. 5),[54,55] in contrast to the true six-centered delocalization in benzene. Natural bond orbital (NBO) analyses also indicate that B–O bonds in the B_3O_3 boroxol cores in both **1** and **3** are highly polarized, with net atomic charges of q_B = +0.82, +0.98 |e|, and q_O = −0.85, −0.87 |e| for **1** and **3**, respectively. Thus, there exists a negative-positive alternation in charge distribution of the B_3O_3 boroxol cores and the circular delocalization (and hence aromaticity) in **1** and **3** should be substantially reduced.

To further elucidate the nature of bonding, we performed the AdNDP analysis[34] for $B_3O_3(BO)_3$ (**1**). The results are straightforward and easy to interpret (Fig. 6). Of the 54 valence electrons in total, 12 are for the O 2s/2p lone pairs, either terminal or bridging; 18 are for three terminal B≡O triple bonds; 6 are for three B−BO single bonds; and 12 are for six B−O bonds in B_3O_3 ring. The remaining six electrons are delocalized to form three 6c-2e π bonds (bottom row; Fig. 6), which have the same pattern as that revealed from MO analysis (Fig. 4). It is interesting to point out that although the three O atoms contribute the most to the three 6c-2e π bonds, AdNDP analyses indicate that the π system cannot be further localized into three 1c-2e lone pairs over the three O atoms in the core. This result shows that the relatively small contribution from the three B $2p_z$ atomic orbitals, that is, the covalent nature of B−O π bonding, plays a critical role in defining the nature of delocalized π system. The covalent nature is also apparent in the gas-phase BO radical.

B. NRT and NICS analyses

Natural resonance theory (NRT) is used to shed further light on the difference between benzene and its inorganic analogs: boronyl boroxine $B_3O_3(BO)_3$ (**1**) and boroxine $B_3O_3H_3$ (**3**). The results are shown in the supplementary material (Fig. S2).[53] Clearly, boronyl boroxine has the leading resonance structure with conjugated π bonds (62%), which shows a gradual increase to 68% and 82%, respectively, in boroxine and benzene. On the other hand, the percentage of the resonance structure with localization of lone pairs on the electronegative atoms decreases from boronyl boroxine (22%) to boroxine (21%), and to benzene (8%). Both trends are consistent with the reduction of electron delocalization (and aromaticity) from benzene to boroxine and

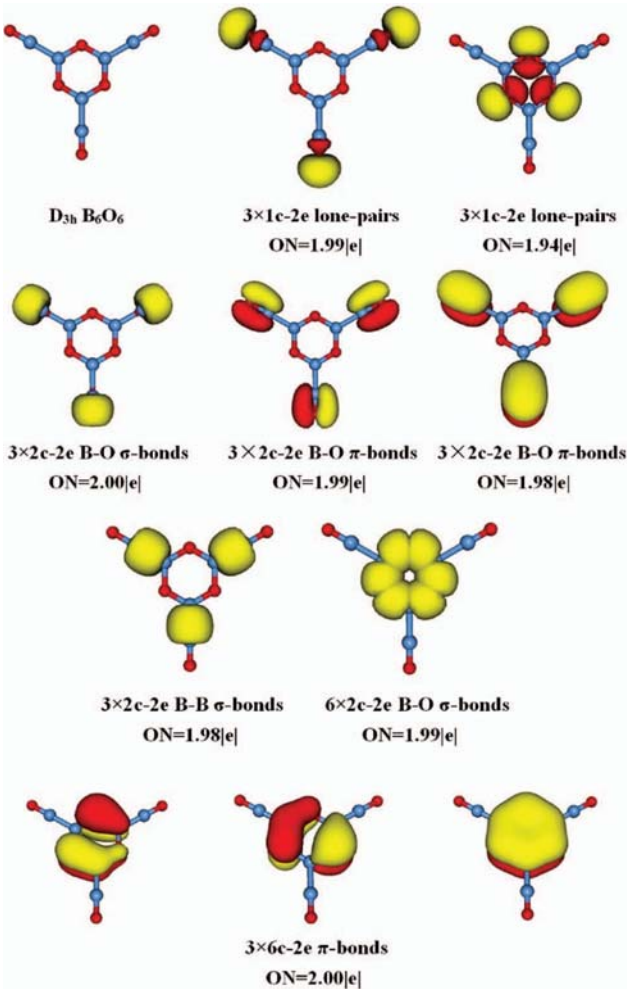

FIG. 6. AdNDP bonding pattern of boronyl boroxine D_{3h} B_6O_6 (**1**, $^1A_1'$). The occupation numbers (ONs) are indicated.

boronyl boroxine, where the latter two have roughly the same properties.

NICS is widely used to quantify the extent of aromaticity, and a negative NICS value denotes aromaticity.[39,40] $NICS_{zz}(1)$ appears to be a better indicator of π aromaticity for planar molecules. The calculated $NICS_{zz}(1)$ values for $B_3O_3(BO)_3$ (**1**) and $B_3O_3H_3$ (**3**) are −2.8 and −3.4 ppm at the molecular center, respectively (Table I). These are negative but relatively small values, which indicate weak π aromaticity in the inorganic benzene species. For comparison, the prototypical aromatic benzene has a $NICS_{zz}(1)$ value of −29.7 ppm at the same level. Overall, the NICS results are qualitatively in line with those of NRT and ELF analyses, confirming boronyl boroxine as a close analog of boroxine, which are both inorganic benzene species.

C. Possible implication of boronyl boroxine on vitreous B_2O_3

Boronyl boroxine D_{3h} $B_3O_3(BO)_3$ (**1**, $^1A_1'$) is simple in structure, yet it contains all critical structural and bonding elements in glassy bulk B_2O_3 and high temperature B_2O_3 liquids: the six-membered B_3O_3 boroxol ring and the terminal BO groups. Amorphous B_2O_3 bulk materials have remained structurally controversial and challenging to model, but it is generally thought that boroxol B_3O_3 ring constitutes a large fraction of them, probably up to 75%.[56] On the other hand, it has long been speculated that the network in B_2O_3 liquids is terminated by boronyl groups, whose population increases with temperature.[57]

The intrinsic stability of boronyl boroxine as a robust gas-phase cluster hints that boroxol B_3O_3 ring is likely the preferred structural building block for boron oxides, which aggregates and networks to form the vitreous B_2O_3 materials. The potency for this relatively small cluster to develop a boroxol B_3O_3 ring core structure that dominates the glassy and liquid B_2O_3 phases is remarkable, and indeed surprising. Boronyl boroxine and similar larger clusters may thus be interesting molecules to mimic the microscopic, short-range structures of amorphous B_2O_3 glasses and liquids, and to model their nucleation and growth.

D. Predicted electronic properties for boronyl boroxine and its anion

To aid future experimental characterizations of boronyl boroxine and its anion, we report herein their calculated electronic properties. Ionization potentials (IPs) are calculated at B3LYP/6-311+G(d,p) level for boronyl boroxine $B_3O_3(BO)_3$ (**1**), boroxine $B_3O_3H_3$ (**3**), and benzene, which are 12.22,

TABLE I. Natural atomic charges q_M (|e|), lowest vibrational frequencies ν_{min} (cm^{-1}), HOMO-LUMO energy gaps (ΔE_{Gap}, in eV), electron affinities (EA, in eV), and ionization potentials (IP, in eV) of D_{3h} $B_3O_3(BO)_3$ (**1**) and its $[B_3O_3(BO)_3]_2Cr$ (**4**) sandwich complex at the B3LYP/6-311+G(d,p) level, as compared with those of D_{3h} $B_3O_3H_3$ (**3**). $NICS_{zz}(1)$ values are also listed for **1**, **3**, and benzene.

Species	State	q_M[a,b]	ν_{min}	ΔE_{Gap}[c,d]	EA[e]	IP	$NICS_{zz}(1)$
D_{3h} $B_3O_3(BO)_3$ (**1**)	$^1A_1'$		62	7.05	1.82	12.22	−2.8
D_{3d} $[B_3O_3(BO)_3]_2Cr$ (**4**)	^1A_g	0.28	25	3.22			
D_{3h} $B_3O_3H_3$ (**3**)	$^1A_1'$		213	8.49	−0.57	11.87	−3.4
D_{6h} C_6H_6	$^1A_{1g}$		411	6.60		9.28	−29.7

[a]Charge on the metal center via natural bond orbital (NBO) analysis.
[b]Charge on the Cr center in D_{3d} $[B_3O_3H_3]_2Cr$ (**5**) is +0.20 |e|.
[c]Calculated as orbital energy difference between the HOMO and the LUMO.
[d]ΔE_{Gap} for D_{3d} $[B_3O_3H_3]_2Cr$ (**5**) is 3.70 eV.
[e]More accurate EA values at the CCSD(T)//B3LYP/6-311+G(d,p) level are 1.17, −0.85, and −1.81 eV for D_{3h} $B_3O_3(BO)_3$ (**1**), D_{3h} $B_3O_3H_3$ (**3**), and D_{6h} C_6H_6, respectively. See text for discussion.

11.87, and 9.28 eV, respectively (Table I). Boronyl boroxine is thus predicted to have an IP that is comparable to and slightly greater than boroxine, which are both substantially higher than that of benzene (by ∼2.6−2.9 eV), suggesting that boronyl boroxine is a relatively stable neutral species. These IP values at B3LYP appear to be quite reliable, in light of the fact that the calculated IP for benzene is in excellent agreement with the most recent, accurate experimental data (9.24384 ± 0.00006 eV).[58]

With one electron attached, the C_{2v} $B_3O_3(BO)_3^-$ (**2**, $^2A_2$) anion cluster is produced (Fig. 1). The extra electron in **2** occupies one of the degenerate LUMO (e″) oribtals of **1**, resulting in a slight Jahn-Teller distortion in the anion from the perfect D_{3h} structure. The terminal BO groups in **2** retain their boronyl nature ($r_{B\equiv O}$ = 1.21−1.22 Å). The ground-state adiabatic and vertical detachment energies (ADE and VDE) of **2** are predicted at B3LYP/6-311+G(d,p) level to be ADE = 1.82 and VDE = 2.03 eV, where the ADE also represents electron affinity (EA) of **1** (Table I). The simulated photoelectron spectrum based on B3LYP/6-311+G(d,p) and time-dependent DFT (TDDFT)[59,60] calculations are depicted in Fig. S3 in the supplementary material,[53] which exhibits a huge energy gap between its ground-state band (X) and first excited-state band (A), amounting to 4.83 eV at the TDDFT level. The X−A gap of an anion is a rough reflection of the HOMO-LUMO gap of a closed-shell neutral species. Thus, the simulated photoelectron spectrum further suggests that B_6O_6 (**1**) is an extraordinarily stable species. Indeed, B3LYP calculation yields a huge HOMO-LUMO energy gap of 7.05 eV for **1** (Table I). For comparison, the celebrated C_{60} molecule has an X−A energy gap of 1.62 eV as revealed from the photoelectron spectrum of C_{60}^- anion.[61]

It is well known that the EA calculation for an anion is challenging for the DFT methods, including B3LYP. This is particularly true for a stable neutral cluster with a large HOMO-LUMO gap, such as boronyl boroxine (**1**). To address this technical issue, we have run further calculations. First, we checked the EA at B3LYP using the augmented Dunning's all-electron basis sets (aug-cc-pVTZ) that include diffuse functions, which many believe can better handle an anion. We also calculated the EA using different functionals. The results thus obtained are 1.78 eV at B3LYP/aug-cc-pVTZ and 1.81 eV at PBE1PBE/6-311+G(d,p), which are nearly identical to that at B3LYP/6-311+G(d,p). Second, we checked the EA at more sophisticated MO theory levels. The calculated EA values are 1.11 eV at MP2/6-311+G(d,p), 1.17 eV at CCSD(T)//B3LYP/6-311+G(d,p), 1.17 eV at CCSD(T)//PBE1PBE/6-311+G(d,p), and 1.16 eV at CCSD(T)//MP2/6-311+G(d,p). These numbers are remarkably consistent with each other within 0.06 eV, and should be considered to be more reliable than the DFT results. The 0.3–0.6 eV discrepancy between DFT and MO theory in the EAs of boronyl boroxine and boroxine is another example that demonstrates the limitation of DFT methods in certain cases. In summary, the recommended EA for boronyl boroxine D_{3h} $B_3O_3(BO)_3$ (**1**, $^1A_1'$) based on MO theory calculations is 1.1−1.2 eV, which should be compared with further experimental data.

For comparison, the calculated EA values for boroxine (**3**) is −0.85 eV at CCSD(T)//B3LYP/6-311+G(d,p) level, whereas benzene is known to have a negative EA. Thus for the species discussed here, the photoelectron spectroscopy technique is probably suitable only for characterizations of boronyl boroxine and its anion. Note that the EA of **1** is much higher than that of **3** due to the fact that the terminal BO ligand is more electronegative than H, resulting in electrostatic stabilization in **1** relative to **3** by ∼2 eV at CCSD(T) level (∼0.7 eV per BO group). A similar effect was observed in our previous studies on $Au_2(BO)$ versus Au_2H, where the former species has a higher EA (4.32 eV) than the latter (3.55 eV).[62,63]

E. Sandwich-type complexes containing $B_3O_3X_3$ (X = BO, H) units

Motivated by the intriguing electronic and magnetic properties of multidecker organometallic sandwich clusters and their infinite one-dimensional molecular wires, a series of recent works has explored the use of D_{6h} C_6H_6 and D_{3h} $B_3N_3H_6$ as ligands to form multidecker sandwich molecular wires.[64–68] It is thus of interest as well to pursue sandwich-type transition metal complexes by using D_{3h} $B_3O_3(BO)_3$ (**1**) and D_{3h} $B_3O_3H_3$ (**3**) as ligands. Figure 7 shows the optimized structures of D_{3d} $[B_3O_3(BO)_3]_2Cr$ (**4**) and D_{3d} $[B_3O_3H_3]_2Cr$ (**5**) sandwich complexes at the B3LYP level, in which two **1** and **3** ligands, respectively, sandwich one Cr atom from the opposite ends along the threefold axis of the systems, forming staggered D_{3d} complexes with the Cr−B distances of r_{Cr-B} = 2.26 and 2.25 Å in **4** and **5**, respectively. These distances are slightly longer than that in D_{6h} $[C_6H_6]_2Cr$ (**6**): r_{Cr-C} = 2.17 Å. Note that different from the eclipsed **6** sandwich complex,[62–64] the staggered D_{3d} complexes **4** and **5** are true minimum with the lowest vibrational frequency of 25 and 80 cm^{-1}, respectively. The corresponding eclipsed D_{3h} structures of $[B_3O_3X_3]_2Cr$ (X = BO, H) turn out to be transition states with one imaginary frequency due to the electrostatic repulsion between the two ligands, similar to the situation in $[B_3N_3H_6]_2M$.[67,68] The $D_{3d} \rightarrow D_{3h}$ rotatory transition for $[B_3O_3(BO)_3]_2Cr$ and $[B_3O_3H_3]_2Cr$ has an energy barrier of 18.91 and 10.11 kcal/mol, respectively, suggesting that boronyl boroxine based sandwich complex **4** is more robust against rotatory transition relative to its boroxine counterpart **5**.

It is worth noting that both $B_3O_3(BO)_3$ and $B_3O_3H_3$ units in the D_{3d} sandwich complexes are structurally well preserved. For instance, the B−O bond distances in the

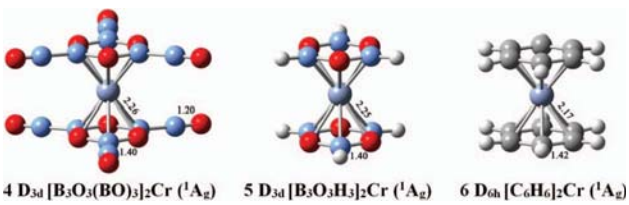

FIG. 7. Sandwich-type D_{3d} $[B_3O_3(BO)_3]_2Cr$ (**4**, ^1A_g) complex at the B3LYP/6-311+G(d,p) level, as compared with its boroxine and benzene counterparts: D_{3d} $[B_3O_3H_3]_2Cr$ (**5**, ^1A_g) and D_{6h} $[C_6H_6]_2Cr$ (**6**, ^1A_g). Selected bond distances (in Å) are labeled. The B atom is in blue, O in red, Cr in pink, and C and H in gray.

B_3O_3 ring in **4** and **5** are 1.40 Å, well comparable to 1.38 Å in **1** and **3**. Also, B≡O bond distance in **4** is 1.20 Å, nearly identical to that either in **1** or the gas-phase BO radical.[21] NBO analyses show that the **4** and **5** sandwich complexes exhibit only slight charge separation as follows: $[B_3O_3(BO)_3]^{-0.14}$-$Cr^{+0.28}$-$[B_3O_3(BO)_3]^{-0.14}$ and $[B_3O_3H_3]^{-0.10}$-$Cr^{+0.20}$-$[B_3O_3H_3]^{-0.10}$. We also note that both sandwich **4** and **5** complexes possess sizeable HOMO-LUMO gaps: 3.22 eV for **4** and 3.70 eV for **5** at the B3LYP level (Table I), suggesting that these complexes are stable species thermodynamically. Preliminary calculations also indicate that such complexes can be extended to form triple-decker sandwich-type structures and to include other transition metal centers.

V. CONCLUSIONS

We report on theoretical prediction of boronyl boroxine, D_{3h} $B_3O_3(BO)_3$ (**1**, $^1A_1'$), which represents a new member of the "inorganic benzene" family. This perfectly planar cluster is identified as the global minimum, via the gradient embedded genetic algorithm, the Coalescence Kick, and the Basin Hopping global-minimum searches. It lies ∼20 kcal/mol lower in energy than the nearest alternative structure at both B3LYP and single-point CCSD(T) levels. Boronyl boroxine closely resembles boroxine D_{3h} $B_3O_3H_3$ (**3**) in structure and bonding, readily obtainable from the latter via isovalent BO/H substitution. Chemical bonding in boronyl boroxine is elucidated using molecular orbital analysis, adaptive natural density partitioning, natural resonance theory, and nucleus independent chemical shift calculations, which consistently reveal weak π aromaticity in boronyl boroxine and render it a true member of the inorganic benzene family. Electronic properties are predicted for D_{3h} $B_3O_3(BO)_3$ (**1**, $^1A_1'$) and its anion C_{2v} $B_3O_3(BO)_3^-$ (**2**, $^2A_2$), which should aid their future experimental characterizations. Boronyl boroxine and similar larger clusters may serve as valuable molecular models for vitreous B_2O_3 glasses and liquids. To explore the potential of boronyl boroxine as a ligand, sandwich-type transition metal complexes, D_{3d} $[B_3O_3(BO)_3]_2Cr$ (**4**) and $[B_3O_3H_3]_2Cr$ (**5**), are designed computationally, which are analogs of the sandwich complexes based on benzene and borazine and may be extended to form multidecker sandwich complexes.

ACKNOWLEDGMENTS

We would like to thank Professor A. I. Boldyrev for the gradient embedded genetic algorithm (GEGA) and the Coalescence Kick (CK) global-minimum search and the adaptive natural density partitioning (AdNDP) programs, and Professor Jun Li for the Basin Hopping global-minimum search program. This work was supported by the National Natural Science Foundation of China (Grant Nos. 20873117 and 21243004).

[1] L. Hanley and S. L. Anderson, J. Chem. Phys. **89**, 2848 (1988).
[2] D. Peiris, A. Lapicki, S. L. Anderson, R. Napora, D. Linder, and M. Page, J. Phys. Chem. A **101**, 9935 (1997).
[3] T. R. Burkholder and L. Andrews, J. Chem. Phys. **95**, 8697 (1991).
[4] M. L. Drummond, V. Meunier, and B. G. Sumpter, J. Phys. Chem. A **111**, 6539 (2007).
[5] X. J. Feng, Y. H. Luo, X. Liang, L. X. Zhao, and T. T. Cao, J. Cluster Sci. **19**, 421 (2008).
[6] T. B. Tai and M. T. Nguyen, Chem. Phys. Lett. **483**, 35 (2009).
[7] M. T. Nguyen, M. H. Matus, V. T. Ngan, D. J. Grant, and D. A. Dixon, J. Phys. Chem. A **113**, 4895 (2009).
[8] T. B. Tai, M. T. Nguyen, and D. A. Dixon, J. Phys. Chem. A **114**, 2893 (2010).
[9] C. B. Shao, L. Jin, and Y. H. Ding, J. Comput. Chem. **32**, 771 (2011).
[10] H. J. Zhai, S. D. Li, and L. S. Wang, J. Am. Chem. Soc. **129**, 9254 (2007).
[11] S. D. Li, H. J. Zhai, and L. S. Wang, J. Am. Chem. Soc. **130**, 2573 (2008).
[12] H. J. Zhai, J. C. Guo, S. D. Li, and L. S. Wang, ChemPhysChem **12**, 2549 (2011).
[13] H. J. Zhai, C. Q. Miao, S. D. Li, and L. S. Wang, J. Phys. Chem. A **114**, 12155 (2010).
[14] H. Bai, H. J. Zhai, S. D. Li, and L. S. Wang, Phys. Chem. Chem. Phys. **15**, 9646 (2013).
[15] Q. Chen, H. J. Zhai, S. D. Li, and L. S. Wang, J. Chem. Phys. **137**, 044307 (2012).
[16] W. Z. Yao, J. C. Guo, H. G. Lu, and S. D. Li, J. Phys. Chem. A **113**, 2561 (2009).
[17] H. Braunschweig, K. Radacki, and A. Schneider, Science **328**, 345 (2010).
[18] R. J. Doyle, J. Am. Chem. Soc. **110**, 4120 (1988).
[19] S. H. Bauer, Chem. Rev. **96**, 1907 (1996).
[20] P. G. Wenthold, J. B. Kim, K. L. Jonas, and W. C. Lineberger, J. Phys. Chem. A **101**, 4472 (1997).
[21] H. J. Zhai, L. M. Wang, S. D. Li, and L. S. Wang, J. Phys. Chem. A **111**, 1030 (2007).
[22] W. N. Lipscomb, Science **196**, 1047 (1977).
[23] S. D. Li, J. C. Guo, and G. M. Ren, J. Mol. Struct.: THEOCHEM **821**, 153 (2007).
[24] C. Q. Miao and S. D. Li, Sci. China Chem. **54**, 756 (2011).
[25] L. Barton, F. A. Grimm, and R. F. Porter, Inorg. Chem. **5**, 2076 (1966).
[26] F. A. Grimm, L. Barton, and R. F. Porter, Inorg. Chem. **7**, 1309 (1968).
[27] C. H. Chang, R. F. Porter, and S. H. Bauer, Inorg. Chem. **8**, 1689 (1969).
[28] J. A. Tossell and P. Lazzeretti, J. Phys. Chem. **94**, 1723 (1990).
[29] K. L. Bhat, G. D. Markham, J. D. Larkin, and C. W. Bock, J. Phys. Chem. A **115**, 7785 (2011).
[30] A. Kaldor and R. F. Porter, Inorg. Chem. **10**, 775 (1971).
[31] S. H. Bauer, J. Am. Chem. Soc. **60**, 524 (1938).
[32] B. L. Crawford and J. T. Edsall, J. Chem. Phys. **7**, 223 (1939).
[33] P. W. Fowler and E. Steiner, J. Phys. Chem. A **101**, 1409 (1997).
[34] D. Yu. Zubarev and A. I. Boldyrev, Phys. Chem. Chem. Phys. **10**, 5207 (2008).
[35] P. v. R. Schleyer, C. Maerker, A. Dransfeld, H. J. Jiao, and N. J. R. E. Hommes, J. Am. Chem. Soc. **118**, 6317 (1996).
[36] P. v. R. Schleyer, H. Jiao, N. J. R. v. E. Hommes, V. G. Malkin, and O. L. Malkina, J. Am. Chem. Soc. **119**, 12669 (1997).
[37] A. N. Alexandrova, A. I. Boldyrev, Y. J. Fu, X. Yang, X. B. Wang, and L. S. Wang, J. Chem. Phys. **121**, 5709 (2004).
[38] A. N. Alexandrova and A. I. Boldyrev, J. Chem. Theory Comput. **1**, 566 (2005).
[39] M. Saunders, J. Comput. Chem. **25**, 621 (2004).
[40] P. P. Bera, K. W. Sattelmeyer, M. Saunders, H. F. Schaefer, and P. v. R. Schleyer, J. Phys. Chem. A **110**, 4287 (2006).
[41] D. J. Wales and J. P. K. Doye, J. Phys. Chem. A **101**, 5111 (1997).
[42] A. D. Becke, J. Chem. Phys. **98**, 5648 (1993).
[43] C. Lee, W. Yang, and R. G. Parr, Phys. Rev. B **37**, 785 (1988).
[44] M. J. Frisch, G. W. Trucks, H. B. Schlegel *et al.*, GAUSSIAN 03, Revision A.l, Gaussian, Inc., Pittsburgh, PA, 2003.
[45] J. A. Pople, M. Head-Gordon, and K. Raghavachari, J. Chem. Phys. **87**, 5968 (1987).
[46] G. E. Scuseria and H. F. Schaefer III, J. Chem. Phys. **90**, 3700 (1989).
[47] G. E. Scuseria, C. L. Janssen, and H. F. Schaefer III, J. Chem. Phys. **89**, 7382 (1988).
[48] J. Cizek, Adv. Chem. Phys. **14**, 35 (1969).
[49] The CP2K developers group, 2000−2011, see http://cp2k.berlios.de/.
[50] J. VandeVondele, M. Krack, F. Mohamed, M. Parrinello, T. Chassaing, and J. Hutter, Comput. Phys. Commun. **167**, 103 (2005).
[51] Stuttgart RSC 1997 ECP basis sets used in this work and the related references therein can be obtained at https://bse.pnl.gov/bse/portal.

[52]E. D. Glendening, J. K. Badenhoop, A. E. Reed, J. E. Carpenter, J. A. Bohmann, C. M. Morales, and F. Weinhold, NBO *5.0* (Theoretical Chemistry Institute, University of Wisconsin, Madison, WI, 2001).
[53]See supplementary material at http://dx.doi.org/10.1063/1.4811330 for the calculated dissociation energies for D_{3h} $B_3O_3(BO)_3$ (**1**) at the B3LYP/6-311+G(d,p) level (Table SI); molecular dynamic simulations of D_{3h} $B_3O_3(BO)_3$ (**1**) at 300K (Figure S1); main resonant structures as revealed from natural resonance theory (NRT) analyses for D_{3h} $B_3O_3(BO)_3$ (**1**), as compared with those for D_{3h} $B_3O_3H_3$ (**3**) and benzene (Figure S2); and simulated photoelectron spectrum of C_{2v} $B_3O_3(BO)_3^-$ (**2**) based on TDDFT calculations (Figure S3).
[54]B. Silvi and A. Savin, Nature (London) **371**, 683 (1994).
[55]J. C. Santos, J. Andres, A. Aizman, and P. Fuentealba, J. Chem. Theory Comput. **1**, 83 (2005).
[56]See for example G. Ferlat, T. Charpentier, A. P. Seitsonen, A. Takada, M. Lazzeri, L. Cormier, G. Calas, and F. Mauri, Phys. Rev. Lett. **101**, 065504 (2008).
[57]J. D. Mackenzie, J. Phys. Chem. **63**, 1875 (1959).
[58]G. I. Nemeth, H. L. Selzle, and E. W. Schlag, Chem. Phys. Lett. **215**, 151 (1993).
[59]M. E. Casida, C. Jamorski, K. C. Casida, and D. R. Salahub, J. Chem. Phys. **108**, 4439 (1998).
[60]R. Bauernschmitt and R. Ahlrichs, Chem. Phys. Lett. **256**, 454 (1996).
[61]X. B. Wang, H. K. Woo, and L. S. Wang, J. Chem. Phys. **123**, 051106 (2005).
[62]D. Yu. Zubarev, A. I. Boldyrev, J. Li, H. J. Zhai, and L. S. Wang, J. Phys. Chem. A **111**, 1648 (2007).
[63]H. J. Zhai, B. Kiran, and L. S. Wang, J. Chem. Phys. **121**, 8231 (2004).
[64]J. L. Wang, L. Y. Zhu, X. Y. Zhang, and M. L. Yang, J. Phys. Chem. A **112**, 8226 (2008).
[65]J. L. Wang, P. H. Acioli, and J. Jellinek, J. Am. Chem. Soc. **127**, 2812 (2005).
[66]H. J. Xiang, J. L. Yang, J. G. Hou, and Q. S. Zhu, J. Am. Chem. Soc. **128**, 2310 (2006).
[67]L. Y. Zhu and J. L. Wang, J. Phys. Chem. C **113**, 8767 (2009).
[68]S. S. Mallajosyula, P. Parida, and S. K. Pati, J. Mater. Chem. **19**, 1761 (2009).